Structure Characterization of Nanocomposites by Synchrotron X-ray Rays

P. Nawani, C. Burger, X. Chen, B. Chu and B. S. Hsiao*

Chemistry Department, Stony Brook University, Stony Brook, New York 11794-3400.

ABSTRACT

The two most routinely used characterization techniques for determination of nanofiller morphology (e.g. exfoliation and intercalation of nanoclays, orientation of nanotubes) in polymer nanocomposites are transmission electron microscopy (TEM) and small-angle X-ray scattering (SAXS). The latter can be further used for in-situ and time-resolved studies. In this paper, we demonstrate that the use of three-dimension (3D) TEM and novel SAXS analysis can provide quantitative and complimentary structural information about clay orientation in polymer nanocomposites. In another part of the study, crystallization of model polyethylene blends (UHMWPE and low molecular weight polyethylene (MB-50k)) containing multi-walled carbon nanotubes (MWNT) was investigated by using in-situ rheo-X-ray techniques combining rheological and structural properties. The role of MWNT on the crystallization of model polyethylene blends at different temperature is discussed.

Keywords: Organoclay, carbon nanotubes, polymer nanocomposite, SAXS, TEM

1. INTRODUCTION

The state of nanofiller dispersion and orientation has long been an essential issue in polymer nanocomposites, affecting many physical properties from mechanical moduli to gas permeability [1,2]. However, extracting information about the nanofiller dispersion and orientation using these techniques requires a certain degree of careful data analysis, not commonly practiced in the community. For example, quantitative analysis of TEM has been shown to be capable of evaluating the extent of layered silicate exfoliation in polymer matrices [3]

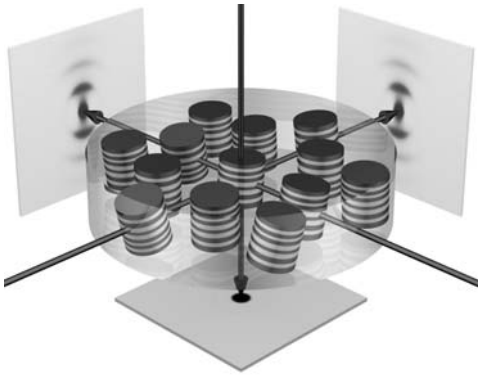

Figure 1. Directional SAXS simulation from nanoclays with cylindrical symmetry and preferred orientations.

In this paper, we demonstrate that directional 2D SAXS techniques can provide the spatial distribution and an estimate of the orientation state of nanoclays in nanocomposites (Figure 1). The chosen model nanocomposite system was based on melt mixed ethylene-vinyl acetate (EVA) copolymers and organoclays (cloisite, C20A) [4]. Furthermore, multiple scattering peaks were observed in SAXS profiles of neat organoclay and the appearance of non-equidistant SAXS maxima could be attributed to the presence of bimodal layer thickness distributions of the organic layers in organoclays [5].

In another study, nanocomposites based on modified multi-walled carbon nanotubes (MWNT) were studied using combined SAXS, wide-angle X-ray diffraction (WAXD) and rheology techniques. It is well known that long chains are primarily responsible for the formation of the crystallization precursor structure, especially the shish, under flow [6,7]. However, network-like precursor structures can also be manipulated by the addition of interpenetrating networks and nano-scale particles such as carbon nanotubes. The effects of MWNT in our model UHMWPE/MB50k blend thus provide important structure information on developing a new type of very tough MWNT/UHMWPE nanocomposite fiber.

2. EXPERIMENT

2.1 Materials and Preparation

The chosen clay materials included Cloisite® 20 (C20A) organoclay, manufactured by Southern Clay Company. Based on the data provided by Southern Clay, C20A contained montmorillonite (Wyoming cloisite) and di-methyl di-hydrogenated tallow quaternary ammonium chloride (DMDTA) as organic surfactant. The content of the surfactant in C20A organoclay was 35 wt%. DMDTA was a blend of surfactants prepared from natural products by Akzo Nobel. According to Akzo Nobel, the major component in this blend was di-methyl di-octadecyl-ammonia chloride (DMDOA); minor components included (in the order of decreasing content) di-methyl octadecyl – hexadecylammonia chloride, di-methyl di-hexadecyl ammonium chloride, and a small (<3 wt%) amount of tertiary ammonium chlorides (such as di-methyl octadecyl ammonium chloride and di-methyl – hexadecyl ammonium chloride). To prepare polymer organoclay nanocomposites, the polymer used was EVA8 (ethylene vinyl acetate), with 8 mol% of vinylacetate; Mw=110 Kg/mol; Mw/Mn~6.0 [4]. The carbon nanotubes used to prepare polymer nanocomposites were octadecylamide modified multi-walled carbon nanotubes (MWNT, 0.8 wt% and 5 wt. %),

having a layer of octadecylamide on the surface. The polymer used in this case was blend of a 2 mol % hexene copolymer of ethylene (Mw = 50,000, also called MB-50k in this paper) and 2 wt% ultra-high molecular weight polyethylene (UHMWPE, Mw = 5-6 x 10^6, MWD ~ 9) [8].

2.2. Transmission Electron Microscopy

All nanocomposite samples were cryo-microtomed at -150 ^oC using a diamond knife to obtain sections of 100 nm thicknesses for TEM measurements. No staining was applied. 2D TEM images were acquired on a JEOL 2000FX TEM instrument at 160 kV accelerating voltage. Multiple images from various locations at different magnifications were collected to provide an overall assessment of the dispersion uniformity. For 3D TEM, a FEI Tecnai TEM instrument (G2 F20 Super Twin TMP) was used. All samples were run on the scanning transmission electron microscopy high-angle annular dark field (STEM-HAADF) mode to minimize the sample damage while maximizing the contrast. The image acquired in such a way is also known as STEM-HAADF tomography. During the measurement, the sample was tilted from a 0 degree angle to -60 degrees, which took about 90 min, and the samples were tilted back from 0 to 60 degrees, which took another 90 min. The total exposure time was 3 hours. The images were reconstructed using the Voltex 3D volume rendering software.

2.3. X-Ray Scattering/Diffraction

Simultaneous small-angle X-ray scattering (SAXS) and wide-angle X-ray diffraction (WAXD) measurements were carried out at the X27C beamline in the National Synchrotron Light Source (NSLS), Brookhaven National laboratory (BNL). The X-ray wavelength used was 0.1366 nm, collimated by a three-pinhole collimation system. SAXS/WAXD images were acquired using image plates manufactured by Fuji Company. 1-D patterns were obtained by integrating 2D images using the Polar software developed at Stony Brook Technology and Applied Research (Stony Brook, NY). The sample-to-detector distances for SAXS was 840 mm and for WAXD was 130 mm. The scattering angle in SAXS was calibrated by a silver behenate standard and the diffraction angle in WAXD was calibrated by an Al_2O_3 standard from the National Institute of Standards and Technology. All scattering/diffraction signals were corrected for beam fluctuations, sample absorption and background scattering.

2.4. Rheology

Rheological measurements were performed using a Physica MCR301 rheometer (Anton Paar Inc., Austria) to determine the viscoelastic behavior of nanocomposites in the molten state. A 25 mm parallel plate fixture was used and small strain oscillatory shear measurements were carried out at 140 ^oC. A constant strain amplitude (γ = 1 %) was employed in all dynamic measurements. The range of the chosen frequency scan was $0.005 < \omega < 100$. The rheo-X-ray measurements using Linkam shear stage followed the protocol as given in the reference [8]

3. RESULTS

3.1. SAXS Analysis of Organoclays

Figure 2 exhibits a selected integrated SAXS profile acquired at room temperature for organoclay C20A. It is interesting to see that the SAXS profiles at room temperature shows multiple peaks, but they do not appear at equidistant positions on the *s* scale. This feature is characteristic of the so-called interstratified system, where multiple layers of different thickness can coexist in the same clay stack as shown in Figure 3.

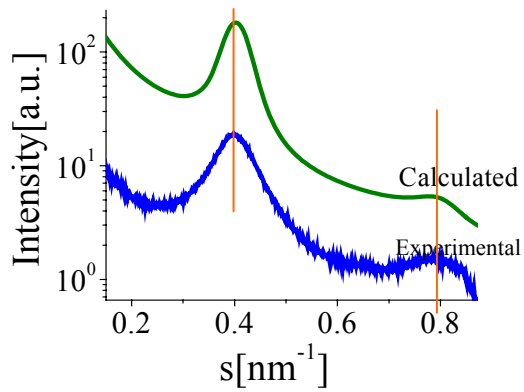

Figure 2. SAXS of organoclay C20A

Results of our SAXS modeling given in detail elsewhere [5] suggest that there exist two populations of organic layers and the thinner layer of thickness 2.6 nm represents the structure of a monolayer of surfactant molecules bound to the adjacent mineral surfaces as shown in Figure 3. The monolayer structure is due to the hydrophobic aggregation of surfactant tails in the organic layers. The thicker organic layer of thickness 5.2 nm consists of two monolayers of surfactant (termed the double-layered structure) with about half of them bound to the mineral surfaces. The free (non-bound) surfactant molecules are held in the silicate gallery by van der Waals forces through aggregations of the hydrophobic tails.

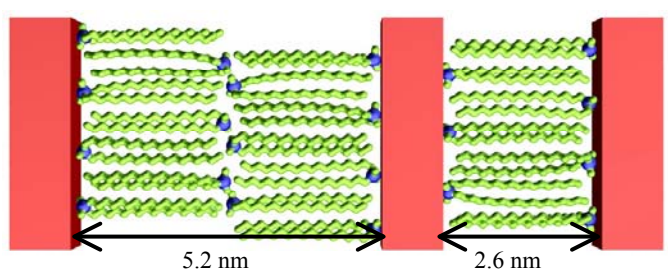

Figure 3. Distribution of surfactants in organoclays

3.2. TEM Observation of Nanocomposites

TEM micrographs of EVA organoclay nanocomposites are illustrated in Figure 4a, showing the organoclay morphology in the polymer matrix.

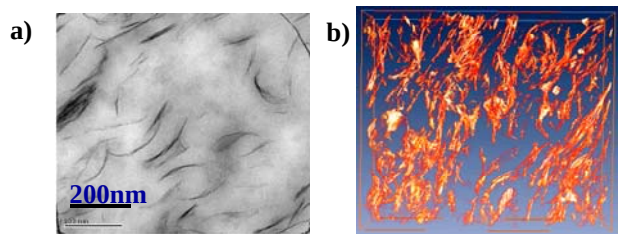

Figure 4: a) 2D TEM and b) 3D TEM, of polymer organoclay nanocomposites

Excellent spatial resolution with a clear definition of the layered structure in intercalated C20A could be seen in these micrographs. Figure 4b shows the 3D TEM image of cryo-microtomed EVA/C20A (10 wt%) nanocomposite samples with a thickness of about 100 nm. The examined 3D volume was 1.6 x 1.6 x 0.1 micron. The 3D TEM view of the extracted clay phase provides a good estimate of the dispersion state of organoclays in the bulk sample. It is clear that the clay stacks were not completely exfoliated in these nanocomposites, which is in accordance with the SAXS data, indicating the existence intercalated stacks

3.3. Directional SAXS Investigation of Polymer Organoclays Nanocomposites:

In SAXS profiles of polymer nanocomposites with organoclay C20A, the scattering peaks shown in Figure 5 are non-equidistant on the *s*-scale, indicating a bimodal distribution of the organic layer [5]. The corresponding SAXS patterns collected along two sample orientations (face-on and edge-on views) confirmed that intercalated clays were oriented parallel to the film plane. Assuming a simple cylindrical symmetry, the orientation of the organoclay particles in the polymer matrix can be fully described by an orientation distribution function g (β) with β being defined as the angle between the normal of organoclay stack and the normal of the film plane.

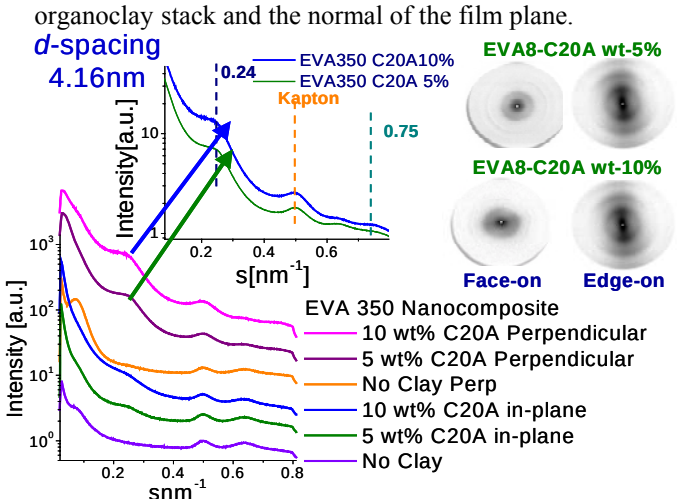

Figure 5. SAXS of polymer organoclay nanocomposites

The meridional maxima of an azimuthal scanning profile for the lamellar stacks would be approximately equivalent to the orientation distribution factor, for which we assume a modified Onsager shape. The corresponding SAXS patterns collected along two sample orientations (face-on and edge-on views) confirmed that intercalated clays were oriented parallel to the film plane. The orientation of clay particles can be fully described by an orientation distribution function *g(β)* with *β* being defined as the angle between the normal of organoclay stack and the normal of the film plane. The Azimuthal scanning profile for the lamellar stacks can thus be expressed by a modified Onsager orientation distribution function:

$$g(\beta) = P_0 + (1-P_0)*(P/\sinh P)*(\cosh(P\cos\beta)) \qquad (1)$$

The extent of the preferred orientation of these clay stacks can calculated using Hermans' orientation parameter:

$$\overline{P}_2 = 0.5*[3*\int_0^{\pi/2} g(\beta)\cos^2(\beta)\sin(\beta)d\beta - 1] \qquad (2)$$

Based on the Eqs (1) and (2), 3D SAXS modeling of clay stacks in nanocomposites can be calculated using the Hermans' orientation parameter expressed as follows.

$$\overline{P}_2 = (1-P_0)(1-3p^{-1}[\coth(p) - p^{-1}]) \qquad (3)$$

In this study, the relationship between orientations of the organoclays and the weight fraction of organoclays (C20A) added in the polymer matrix (EVA) was estimated. From the result for orientation distribution it was observed that higher weight fractions of organoclays led to higher degrees of preferred orientation, which is plausible because less volume is available for the rotation of the organoclay.

3.4. Rheological Investigation of Polymer MWNT Nanocomposites:

The high aspect ratio and superior mechanical strength of MWNT dramatically altered the rheological properties of UHMWPE/MB-50K, as one might expect.

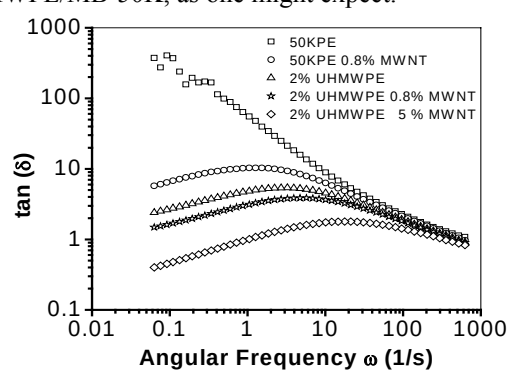

Figure 6. Tan δ (dynamic) of MWNT PE nanocomposites.

Figure 6 shows the damping factor, tan δ, as a function of frequency in the range of 0.05 < ω < 628. The tan δ(ω) curves for the pure MB-50K exhibited a negative slope in

NSTI-Nanotech 2007, www.nsti.org, ISBN 1420061828 Vol. 1, 2007

the entire tested frequency range, indicating the liquid-like melt behavior. In contrast, the 0.8 wt% modified MWNTs/MB-50K nanocomposite melt exhibited a positive slope at low frequency, revealing that a physical network structure due to the presence of modified MWNTs must have been formed in the polyethylene matrix.

3.5.WAXD Investigation of Polymer MWNT Nanocomposites:

Figure 7 shows the WAXD patterns of MWNT/UHMWPE/MB-50k blends at 120 ^{o}C obtained by Linkam shear stage-technique. The WAXD patterns of 2 wt% UHMWPE/MB-50k shows four-arc (110) reflections on the off-axes and two-arc (200) reflections on the meridian, implying the formation of twisted lamellae. Such a kind of twisted lamellae was also found in shear-induced crystallization of HDPE [9]. The possible mechanism may be due to the epitaxial growth of folded chains from the *c*-axis of the flow-induced row nuclei (shish). With the addition of MWNT in 2-wt% UHMWPE blend, it was found that MWNT act as additional nuclei to induce further polyethylene crystallization. The WAXD patterns were significantly different from that the 2-wt% UHMWPE sample where the (200) reflections were changed into the four peaks pattern, indicating that the system possessed a c-axial orientation.

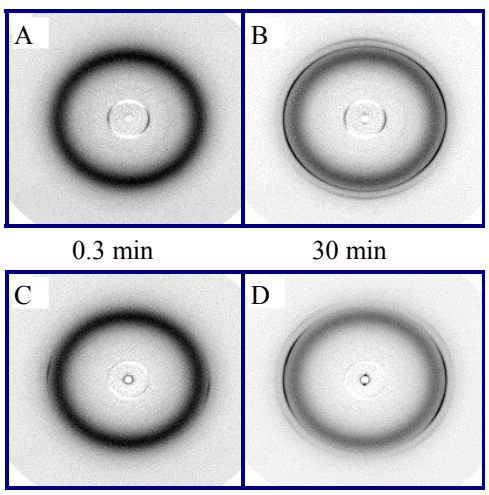

Figure 7. WAXD results from Linkam shear stage at 120 ^{o}C, shear duration 5s. Shear rate = 15 s^{-1}, A and B 2% UHMWPE/50KPE blend: C and D 0.8 % MWNT/2%UHMWPE/50KPE blend.

At 128 ^{o}C, MWNT could not induce crystallization of MB-50k even at a high shear rate of 60 s^{-1}, as seen in the WAXD pattern of 0.8 wt% MWNT/MB-50k blend (data not shown here). However, under the same conditions, the long chain of UHMWPE can crystallize and formed orientated crystal structure in the flow direction (Figure 3). The (110) reflection was narrow for 0.8 wt% MWNT/2 wt%UHMWPE/MB-50k blend system, indicating a highly orientated crystalline structure by SAXS measurements at 128 ^{o}C and shear rate of 60 s^{-1}. The WAXD pattern of 0.8 wt% MWNT/MB-50k blend system was very similar to that of an amorphous melt; confirming that MWNTs cannot induce the crystallization at 128 ^{o}C even at high shear rate of 60 s^{-1}. The SAXS patterns of 2 wt%UHMWPE/MB-50k blend system and 0.8 wt% MWNT/2 wt%UHMWPE/MB-50k blend system were similar. Both exhibited the strong equatorial streak and meridional maxima, due to the shish-kebab structure formed in both blends.

CONCLUSION

Directional SAXS and 3D TEM techniques demonstrate complementary and consistent structure information of polymer nanocomposites. The results show that most organoclays dispersed in a polymer matrix are only partially exfoliated, where organoclays can break into small tactoids with preferred orientation under compression molding. Hermans' orientation factor was calculated and it was found that the extent of orientation of organoclay in the polymer matrix was dependent on its weight percent. The organoclay tactoids are oriented in direction parallel to the surface of the polymer film, which might be due to rotation of organoclays during compression. Due to the interaction/entanglement with MWNTs and long relaxation time of the high molecular weight chains, the orientation of the chain segments in the surrounding of MWNTs cannot relax back to the random coil state as quickly as that in the pure UHMWPE matrix. Thus, the localized orientation of the chains remains strong, which kinetically favors the formation of shish precursors. Since the degree of orientation of the localized shish structures with respect to the flow direction is very high, the shish-induced crystals (including kebabs) also have high degree of orientation (perpendicular to the flow direction).

REFERENCES

[1] E.O. Giannelis, R.Krishnamoorti, E.Manias, ***Adv Polymer Sci 138***, 1999, 107.
[2] M. Alexandre, P. Dubois, ***Mater Sci Eng* 28** 2000, 1.
[3] E. Manias, A. Touny, L. Wu, K. Strawhecker, B. Lu, and T. C. Chung, ***Chem. Mater. 13***, 2001, 3516.
[4] P.Nawani, P.Desai, M.Lundwall, M.Y.Gelfer, B. S. Hsiao, M. Rafailovich, A. Frenkel, A. H. Tsou, J. W. Gilman, S. Khalid ***Polymer, 48***, 2007, 827.
[5] M. Gelfer, C. Burger, A. Fadeev, I. Sics, B.Chu, B.S.Hsiao, A. Heintz, K. Kojo, S-L Hsu, M Si, and M.Rafailovich, ***Langmuir***, **20,** 2004, 3746.
[6] R.H.Somani, L.Yang, L. Zhu, B.S. Hsiao, ***Polymer*** *(feature article)*, **46**, 2005 8587.
[7] B. S. Hsiao, L. Yang, R. H. Somani, C. Avila-Orta, and L. Zhu, ***Phys. Rev. Lett.,* 94**, 2005, 117802.
[8] L. Yang, R.H. Somani, I. Sics, B.S.Hsiao, R. Kolb, H. Fruitwala, C.Ong, ***Macromolecules, 37***, 2004 4845.
[9] J.K.Keum, R.H. Somani, F. Zuo, C. Burger, I.Sics, B.S. Hsiao, H.Chen, R. Kolb, C.T.Lue, ***Macromolecules, 38,*** 2005, 5128.